



Study of Nanoparticle Diffusion in Capillary-Tissue Exchange System using Jeffrey Nanofluid Model: Effects of Shapes of Nanoparticles

Rekha Bali¹, Bhawini Prasad^{1,*}

¹ Department Of Mathematics, School of Basic & Applied Sciences, Harcourt Butler Technical University, Kanpur- 208002, U.P., India

ARTICLE INFO

Article history:

Received 3 December 2022

Received in revised form 4 January 2023

Accepted 3 February 2023

Available online 1 June 2023

Keywords:

Diffusion; Jeffrey Nanofluid; Taylor's Dispersion Model

ABSTRACT

The present work concerns the diffusion of nanoparticles in capillary-tissue exchange system. Nanoparticle are inoculated into the patient's body by intertumoral administration. Thus, nanoparticles diffuse into tumoral tissues through diseased capillary walls. Blood in the capillaries is modelled as Jeffrey fluid. The resultant fluid is called Jeffrey nanofluid. In this model we have described diffusion occurring through the capillary walls into the surrounding tissue. The mathematical results are obtained analytically and have been compared with numerical solution. Graphs have been plotted using MATLAB. The effects of shape factor of nanoparticles, volume fraction of nanoparticles, Jeffrey fluid parameter, viscosity index and viscosity parameter has been observed on velocity and concentration of nanoparticles diffusing into the tissues. A noticeable observation states that brick shaped nanoparticles diffuse most rapidly i.e., have higher diffusion rates than other shapes

1. Introduction

Diffusion is the process by which matter is transported from one part of a system to another as a result of random molecular motions. Biological processes mostly depend on diffusion for transport within cells and tissues. Thus, understanding nanoparticle diffusion in biological systems is an important field of research. Nanoparticles have shown many benefits in their therapeutic applications because of their enhanced abilities of diffusion through viscous biological fluids like mucus. The problem of nanoparticle diffusion in capillary-tissue exchange system is important as it investigates how the nanoparticles seep into the tissues after being injected in the blood. The diffusion of any substance like, nutrient, drug or oxygen in the physiological system is chiefly affected by their diffusion in capillaries [1]. This diffusion of nanoparticles into the tumoral tissues of diseased capillaries can be described by the phenomenon of capillary-tissue exchange system. So, it very important to measure the concentration of nanoparticles diffusing in them. Besides, study of such radial diffusion has vast applications in designing artificial devices which function in extra corporeal circulation [2].

* Corresponding author.

E-mail address: jayabhawini@gmail.com (Bhawini Prasad)

Capillary-tissue exchange occurs in capillary beds where blood is in close proximity to the tissue that surrounds a particular organ [3]. This exchange takes place through the capillary walls. Capillaries are the foremost site of mass transfer between blood and tissue owing to their large surface area. The capillary walls are permeable and abide by the phenomenology of membrane transport. The outer lining of the vessel walls, in cases of some afflictions, may develop tumors under the effect of cholesterol, cellular waste products, lipids, calcium or other substances. The elevated metabolic activity required to develop and grow such depositions are supplied by the underlying cells. As a result, the endothelial cells proliferate rapidly and form unusual tumor like structures that are malignant as seen in tumors surrounding the capillaries in a particular organ. The leaky vasculature due to increased levels of oxygen and nutrient supply, allows drugs to seep into the interstitial tissues. A stunted lymphatic drainage system also intensifies accumulation and local concentration of drugs.

Pharmokinetics defines the bio-availability of drugs by which the drug is absorbed into the tissues. Bio-availability is hence the measurement of drug efficacy. Nanoparticles have manifested themselves as an efficacious approach for the treatment of tumoral diseases like cancer and various cardio vascular blockages. Nanoparticle based targeted drug delivery or nanodrugs aim at commuting drugs to the diseased site in effective concentrations. Nanotechnology offers promising therapeutical effects than conventional methods, considerably reducing the side effects [4]. Nanoparticles are inoculated into the patient's body by intertumoral administration. The success of this administration depends on the effective concentration of nanoparticles that diffuse from the capillaries into the surrounding tissue. Thus, it is significant to study the pharmokinetics and distribution of nanoparticles in the body after nanoparticle administration, in order to achieve the desired outcome.

Nanoparticles have their transport severely hindered in normal vasculature that can cross the vessels walls of tumor vasculatures if they are not at sizes close to or exceeding the pore sizes of the tumour vasculature. Leaky vasculatures have reduced osmotic pressures since nutrients and oxygen can easily pass across the vessel walls leaving the effective pressure equivalent to the vessel pressure. Therefore, leaky tumours with large interstitial fluid pressures are equivalent to the blood pressure. Without any differences between fluid pressures across the capillary vessel wall, nanoparticles are left with diffusion as the only mode of transport through the tumour.

When nanoparticles are dispersed in a base fluid like oil, water, ethylene glycol mixture the fluid is called nanofluid [5]. Nanofluids show enhanced thermophysical properties [33] like thermal conductivity, viscosity, density compared to their respective base fluids in which they are dispersed [6-10]. The behavior of nanofluids is highly governed by the behavior of base fluid. Here, we have considered nanoparticles dispersed in blood. Therefore, blood is the base fluid here.

Blood in diseased blood vessels display non-Newtonian characteristics. Blood flow depicts high shear rates in small blood vessels like capillaries. In such cases blood flow patterns can be described closely using Jeffrey fluid. Jeffrey fluid is a kind of non-Newtonian fluid with shear thinning property. With the increase in shear rate the viscosity of Jeffrey fluid reduces. Ellahi *et al.*, [11] dealt with a mathematical model of Jeffrey fluid in the presence of nanoparticles in tapered stenosed artery having a catheter. Rahman *et al.*, [12] examined the Jeffrey fluid flow with nanoparticles in tapered stenosed artery. Motivated by these, we have thus modelled blood or base fluid as Jeffrey fluid in capillary surrounded by tumoral tissues. The resultant fluid is called as Jeffrey nanofluid.

The diffusion of various substances between capillaries and the surrounding tissues has been studied extensively by numerous investigators both theoretically and experimentally. Krogh's model [13] for the molecular transport between blood capillaries and surrounding tissue cylinder was the first mathematical model used popularly in physiological studies. Popel [14] gave the solution of the diffusion transport in a capillary network and surrounding tissue. He formulated a Neumann- type boundary value problem in a rectangular domain. Blum [15] added a finitely permeable or semi-

permeable membrane capillary wall to Krogh's problem. Levitt [16] attempted to consider diffusional and time dependent interaction of adjacent capillaries. Tandon *et al.*, [17] studied the capillary-tissue fluid exchange system imbibing the characteristics of boundary and medium in which the fluid flows. They showed that filtration from a cylindrical capillary decreased as the step velocity of the porous boundary increases. Tandon and Agarwal [3] studied the diffusion phenomenon in normal and stenotic capillary-tissue fluid exchange system. Diffusivity of nutrients is higher in capillary region compared to that in the tissue region. Siddiqui and Mishra [18] studied the diffusion phenomenon in normal and stenotic capillary-tissue exchange system modelling blood as a modified Casson's fluid. The severity of the stenosis was given due attention using retention parameter. Singh [19] modelled the diffusion phenomenon in stenosed capillary-tissue exchange system using Power law fluid by numerical computations. Bali *et al.*, [20] studied two-layer model of blood in capillary-tissue exchange system. The permeability of the tissue was taken into account for calculating the viscosity and haematocrit. Qiu [1] modelled diffusion process in capillary-tissue system using Krogh's cylinder model. The nature of flow depended on the values of resistance of plasma in extravascular space and the capillary. Ismaeel *et al.*, [21] analysed the heat transfer in capillary-tissue exchange system modelling blood as a nanofluid. This model incorporates the effects of Brownian motion and thermophoresis parameter. They showed that nanoparticle transport across the tissue depended largely on the thermophoresis parameter.

The diffusion of nanoparticles in blood is particularly necessary to comprehend drug delivery. Mun *et al.*, [22] studied the diffusion of nanoparticles in polymer solutions of different types and revealed that geometry of nanoparticle [23, 25], the viscosity of base fluid [26, 32] and the interactions of the nanoparticles with the base fluid strongly effect their diffusivity. Therefore, in this research article we have taken two factors that affect nanoparticle diffusivity i.e., nanoparticle shape and the viscosity of the base fluid.

So far, the phenomenon of diffusion of nanoparticles has been observed mathematically only with respect to their diffusive parameters and not with respect to their shape parameters. Also, the properties of Jeffrey fluid parameters with respect to diffusion in tissues has not been studied. Therefore, in the present article we have made an attempt to provide a detailed examination for diffusion of nanoparticles through the capillary walls into the surrounding diseased tissue. Diffusion occurs through the capillary walls and flow of blood takes place from the arterial end to the venous end. We have assumed that blood in the capillaries with nanoparticles in it as nanofluids. The properties of blood, which is the base fluid, is described by Jeffrey fluid and the resulting fluid is called Jeffrey nanofluid. We have investigated the case of diffusion as nanoparticles seep into the tumoral tissues. The mathematical equations are framed using equation of continuity, Navier-stokes equation and diffusion equation in the capillary and tissue region respectively. Taylor's dispersion model is used to solve the diffusion equation. The equations are solved analytically and numerically by using finite difference method. The obtained results have been compared. The impact of shape of nanoparticles, their volume fraction has been observed on velocity of nanofluid and concentration of nanoparticles. The effects of Jeffrey fluid parameters have also been observed on the same. The graphs have been plotted using MATLAB. The obtained results have useful applications in the field of nano bio-medicine.

2. Mathematical Formulation

We consider blood flow in capillary surrounded by tissue of permeability k_0 . The flow through the capillary tube of length L' with radius R_0 is laminar, steady and incompressible (see Figure 1). The nanoparticles permeate from the capillary into the diseased tissues with height h' . The cylindrical co-

ordinates (r', θ', z') are taken into consideration for describing the velocity of nanofluid. In the axial direction i.e., along z' -axis as u' and \bar{u}' describe the axial velocity in the capillary and tissue region respectively, while v' and \bar{v}' describe the radial velocity i.e., along r' -axis for the capillary and tissue region respectively. The velocity along the θ' -direction is zero due to axis-symmetry. μ_{nf} describes the viscosity of nanofluid while μ_f is the viscosity of base fluid which is blood here.

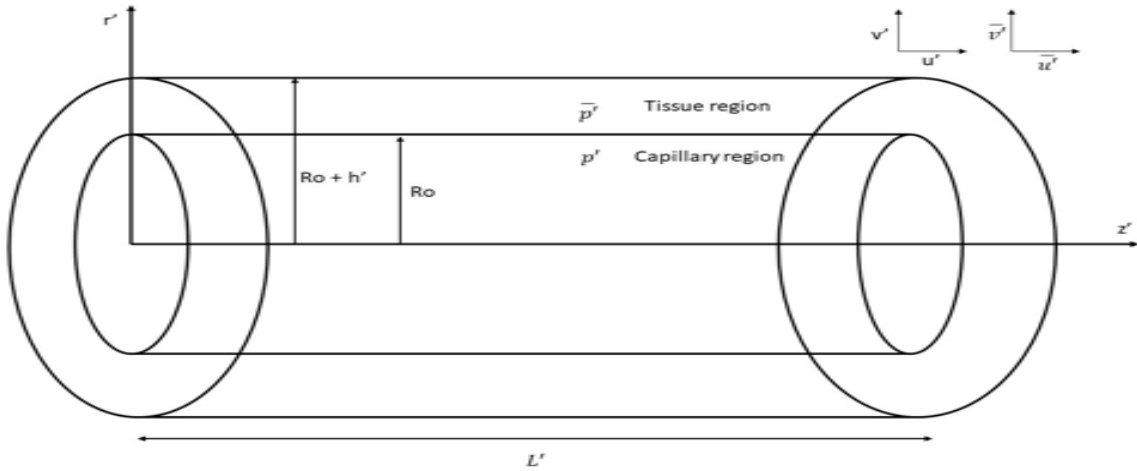


Fig. 1. Geometrical representation of model

The governing equations are given as

Equation of continuity in cylindrical co-ordinates

$$\frac{\partial \rho_{nf}}{\partial t'} = \frac{1}{r'} \frac{\partial (r' \rho_{nf} v')}{\partial r'} + \frac{1}{r'} \frac{\partial \rho_{nf} w'}{\partial \theta'} + \frac{\partial \rho_{nf} u'}{\partial z'} = 0 \tag{1}$$

Navier-Stokes equation in cylindrical co-ordinates

$$\frac{\partial v'}{\partial t'} + v' \frac{\partial v'}{\partial r'} + \frac{u'}{r'} \frac{\partial v'}{\partial \theta'} - \frac{u'^2}{r'} + u' \frac{\partial v'}{\partial z'} = F_{r'} - \frac{1}{\rho_{nf}} \frac{\partial p'}{\partial r'} + \frac{\mu_{nf}}{\rho_{nf}} \left(-\frac{v'}{r'^2} + \frac{1}{r'} \frac{\partial}{\partial r'} \left(r' \frac{\partial v'}{\partial r'} \right) \right) + \frac{1}{r'^2} \frac{\partial^2 v'}{\partial \theta'^2} + \frac{\partial^2 v'}{\partial z'^2} - \frac{2}{r'^2} \frac{\partial w'}{\partial \theta'} \tag{2}$$

$$\frac{\partial w'}{\partial t'} + v' \frac{\partial w'}{\partial r'} + \frac{u'}{r'} \frac{\partial w'}{\partial \theta'} - \frac{v' w'}{r'} + u' \frac{\partial w'}{\partial z'} = F_{\theta'} - \frac{1}{\rho_{nf}} \frac{\partial p'}{\partial \theta'} + \frac{\mu_{nf}}{\rho_{nf}} \left(-\frac{w'}{r'^2} + \frac{1}{r'} \frac{\partial}{\partial r'} \left(r' \frac{\partial w'}{\partial r'} \right) \right) + \frac{1}{r'^2} \frac{\partial^2 w'}{\partial \theta'^2} + \frac{\partial^2 w'}{\partial z'^2} + \frac{2}{r'^2} \frac{\partial v'}{\partial \theta'} \tag{3}$$

$$\frac{\partial u'}{\partial t'} + v' \frac{\partial u'}{\partial r'} + \frac{u'}{r'} \frac{\partial u'}{\partial \theta'} + u' \frac{\partial u'}{\partial z'} = F_{z'} - \frac{1}{\rho_{nf}} \frac{\partial p'}{\partial z'} + \frac{\mu_{nf}}{\rho_{nf}} \left(\frac{1}{r'} \frac{\partial}{\partial r'} \left(r' \frac{\partial u'}{\partial r'} \right) \right) + \frac{1}{r'^2} \frac{\partial^2 u'}{\partial \theta'^2} + \frac{\partial^2 u'}{\partial z'^2} \tag{4}$$

where F in different indices represents body forces with respect to different directions and ρ_{nf} is the density of the nanofluid.

Diffusion equation [34] for nanoparticles in blood in cylindrical co-ordinates

$$\frac{1}{D'} \frac{\partial c'}{\partial t'} + u' \frac{\partial c'}{\partial z'} + v' \frac{\partial c'}{\partial r'} + w' \frac{\partial c'}{\partial \theta'} = \frac{\partial^2 c'}{\partial r'^2} + \frac{1}{r'} \frac{\partial c'}{\partial r'} + \frac{1}{r'^2} \frac{\partial^2 c'}{\partial \theta'^2} + \frac{\partial^2 c'}{\partial z'^2} + m' \tag{5}$$

where D' is diffusivity and m' is the rate of production or degeneration of nanoparticles.

Nanofluids are described as advanced colloidal fluids obtained by the dispersion of 1-100nm nanoparticles in standard fluids. The treatment of viscosity variation in a nanofluid can be considered similar to the effect of viscosity of a solvent by adding solute. Einstein designated the first model for the viscosity in 1906 when he precisely studied the phenomenon of particle diffusion in a dilute solution. Thus, the nanofluid viscosity is described by the equation

$$\mu_{nf} = (1 + A\phi)\mu_f \tag{6}$$

where A is specific to the shape of nanoparticles [23] in the fluid (Table 1) and ϕ is the volume fraction of nanoparticles in blood. μ_f is the viscosity of blood.

The nature of base fluid of a nanofluid largely governs how the nanofluid behaves. Thus, modelling of base fluid is highly important to predict the behavior of nanofluid. Blood is the base fluid in our model, the properties of which are described by a non-Newtonian fluid called the Jeffrey fluid.

The assumption of Newtonian behavior of blood is acceptable for high shear rate flow i.e., while flow through larger blood vessels. It is not valid when the shear rate is low as in the case of capillaries. Class of non-Newtonian fluids having the characteristics memory time scale, also known as the relaxation time scale, also known as the relaxation time, can be will described by Jeffrey fluid model [27, 28]. Jeffrey fluid model is capable of describing the stress-relaxation property of non-Newtonian fluids, which the usual viscous fluid model cannot describe. Jeffrey fluid is specified as a non-Newtonian fluid having shear-thinning property for which the viscosity of fluid reduces with increasing rate of shear stress. λ is the ratio of relaxation to retardation time which is also called Jeffrey fluid parameter, modifying it we get the properties of a Newtonian fluid. Physically, the viscosity of blood is variable i.e., it depends non-linearly on viscosity index and viscosity parameters [2]. Chauhan and Tiwari [2] depicted the importance of Jeffrey fluid with varying viscosity in the dispersion of solutes in blood.

Table 1
 List of shapes of nanoparticles and their respective parameters [23]

Shape of nanoparticles	A (shape parameter)
Platelets	37.1
Blades	14.6
Cylinders	13.5
Bricks	1.9

Thus, combining the effects of nanofluid in Jeffrey fluid is named as Jeffrey nanofluid [29, 30]. The mathematical expression defining shear stress as τ' for Jeffrey nanofluid with varying viscosity [2, 35] is given as:

$$\tau' = \frac{1}{1+\lambda} [\mu_{nf} \{1 + k - k \left(\frac{r'}{R_0}\right)^m\} \left(-\frac{\partial u'}{\partial r'}\right)] \tag{7}$$

where k is the viscosity parameter and m is the viscosity index.

The governing Eq. (1) to Eq. (5) will be solved under the following assumptions:

- I. Flow is considered two dimensional.

- II. Flow is steady in capillaries.
- III. Flow is axisymmetric.
- IV. The azimuthal component of fluid velocity is zero.
- V. The cross-section area is very small in capillaries; thus, the flow is described by low Reynolds number.
- VI. The nanoparticle transfer takes place via diffusion from the capillary to the tissue neglecting the axial diffusion.
- VII. Base fluid is modelled as Jeffrey fluid.

The modified equations for the capillary region and tissue region are given henceforth. The equations in the capillary region ($0 < r' < R_0$)

$$\frac{\partial w'}{\partial z'} + \frac{v'}{r'} + \frac{\partial v'}{\partial r'} = 0 \quad (8)$$

$$\frac{\partial p'}{\partial z'} = -\frac{1}{r'} \frac{\partial}{\partial r'} (r' \tau') \quad (9)$$

where p' is the pressure in the capillary region.

The boundary condition for axis-symmetry of axial flow is expressed as

$$\frac{\partial w'}{\partial r'} = 0 \quad \text{at } r' = 0 \quad (10)$$

Since there is a leakage of nanoparticles from the capillary walls to the tissues, Darcy law is applied at the interface, the boundary condition for which is expressed as

$$u' - \bar{u}' = -\sigma' \frac{\partial w'}{\partial r'} \quad \text{at } r' = R_0 \quad (11)$$

where \bar{p}' is the pressure in the tissue region and σ' is the slip parameter between the capillary and tissue region.

The radial component of velocity is zero at the centre line of nanofluid in the capillary, thus the boundary condition is given as

$$v' = 0 \quad \text{at } r' = 0 \quad (12)$$

Since the fluid permeates from the capillary to the tissues, the boundary condition is expressed as

$$v' = \bar{v}' \quad \text{at } r' = R_0 \quad (13)$$

The boundary conditions for pressure at the capillary ends are expressed as

$$p' = p'_A \quad \text{at } z' = 0 \quad (14)$$

$$p' = p'_B \quad \text{at } z' = L' \quad (15)$$

where p'_A and p'_V is the pressure at the arterial end and venous end.

The diffusion of nanoparticles in the capillary region is given as

$$u' \frac{\partial c'_1}{\partial z'} = D'_1 \left(\frac{\partial^2 c'_1}{\partial r'^2} + \frac{1}{r'} \frac{\partial c'_1}{\partial r'} \right) + m'_1 \quad (16)$$

where c'_1 is the concentration of nanoparticles, D'_1 is the nanoparticle diffusivity and m'_1 is the rate of generation or degeneration of nanoparticles in the capillary region.

The boundary conditions for the diffusion of nanoparticles displaying the axis-symmetry are expressed as

$$\frac{\partial c'_1}{\partial r'} = 0 \quad \text{at } r' = 0 \quad (17)$$

The equations for the tissue region ($R_0 < r' < R_0 + h'$)

Following the Darcy law, the axial and radial components of velocity in the tissue region are given as

$$\bar{u}' = -\frac{k_0}{\mu_{nf}} \frac{\partial \bar{p}'}{\partial z'} \quad \text{and} \quad \bar{v}' = -\frac{k_0}{\mu_{nf}} \frac{\partial \bar{p}'}{\partial r'} \quad (18)$$

Using these in the equation of continuity, we get the Laplace's equation for the pressure distribution in the porous tissue region as

$$\nabla^2 \bar{p}' = 0 \quad (19)$$

No flux condition at the outer wall of the tissue since there is no flow of fluid outside the tissue gives

$$\frac{\partial \bar{p}'}{\partial r'} = 0 \quad \text{at } r' = R_0 + h' \quad (20)$$

The axial pressure gradient at the end points of the tissue is zero which is described as

$$\frac{\partial \bar{p}'}{\partial z'} = 0 \quad \text{at } z' = 0 \quad (21)$$

$$\frac{\partial \bar{p}'}{\partial z'} = 0 \quad \text{at } z' = L' \quad (22)$$

We have considered a matching condition at the tissue and capillary interface

$$\bar{p}' = p' \quad \text{at } r' = R_0 \quad (23)$$

The diffusion equation in the tissue region is given as

$$0 = D'_2 \left(\frac{\partial^2 c'_2}{\partial r'^2} + \frac{1}{r'} \frac{\partial c'_2}{\partial r'} \right) + m'_2 \quad (24)$$

where c'_2 is the concentration of nanoparticles, D'_2 is the nanoparticle diffusivity and m'_2 is the rate of generation or degeneration of nanoparticles in the tissue region.

The no flux condition for diffusion defines the boundary condition as

$$\frac{\partial c'_2}{\partial r'} = 0 \text{ at } r' = R_0 + h' \quad (25)$$

The retention of nanoparticles as they pass from the capillary to the tissue region is given as

$$c'_1 = \delta' c'_2 \text{ at } r' = R_0 \quad (26)$$

where δ' is the retention parameter.

Radial diffusion of nanoparticles as they pass from capillary to the tissue region is given as

$$-D'_1 \frac{\partial c'_1}{\partial r'} = \left(1 - \frac{1}{\delta'}\right) \bar{v}'_{avg} c'_1 - D'_2 \frac{\partial c'_2}{\partial r'} \text{ at } r' = R_0 \quad (27)$$

where \bar{v}'_{avg} is the average radial velocity in the tissue region.

The non-dimensional scheme is stated as:

$$r = \frac{r'}{R_0}, z = \frac{z'}{R_0}, h = \frac{h'}{R_0}, u = \frac{u'}{u_{avg}}, v = \frac{v'}{u_{avg}}, \bar{u} = \frac{\bar{u}'}{u_{avg}}, \bar{v} = \frac{\bar{v}'}{u_{avg}}, \mu_f = \frac{\mu_{nf}}{(1+A\phi)}, L = \frac{L'}{R_0},$$

$$\tau = \frac{\tau' R_0}{\mu_f (1+A\phi) u_{avg}}, \sigma = \frac{\sigma'}{R_0}, p = \frac{p'}{\rho_f u_{avg}^2}, \bar{p} = \frac{\bar{p}'}{\rho_f u_{avg}^2}, Re = \frac{\rho_f u_{avg} R_0}{\mu_f}, D_1 = \frac{D'_1}{D_0}, D_2 = \frac{D'_2}{D_0}, m_1 = \frac{m'_1 R_0^2}{D_0 c_0}, m_2 = \frac{m'_2 R_0^2}{D_0 c_0}, c_1 = \frac{c'_1}{c_0}, c_2 = \frac{c'_2}{c_0}, Pe = \frac{u_{avg} R_0}{D_0}, \delta = \frac{\delta'}{R_0} \quad (28)$$

where u_{avg} is reference velocity, D_0 is reference diffusivity, c_0 is reference concentration. Pe is the Peclet number and Re is the Reynolds number. ρ_f is the density of the blood.

Using the above non-dimensional scheme, the transformed equations are stated as

$$\frac{\partial u}{\partial z} + \frac{v}{r} + \frac{\partial v}{\partial z} = 0 \quad (29)$$

$$\frac{\partial p}{\partial z} = -\frac{1}{Re} \frac{1}{r} \frac{\partial}{\partial r} (r\tau) \quad (30)$$

$$Pe u \frac{\partial c_1}{\partial z} = D_1 \left(\frac{\partial^2 c_1}{\partial r^2} + \frac{1}{r} \frac{\partial c_1}{\partial r} \right) + m_1 \quad (31)$$

$$\nabla^2 \bar{p} = 0 \quad (32)$$

$$0 = D_2 \left(\frac{\partial^2 c_2}{\partial r^2} + \frac{1}{r} \frac{\partial c_2}{\partial r} \right) + m_2 \quad (33)$$

Using the above non-dimensional scheme, the transformed non-dimensional boundary conditions are stated as

$$\frac{\partial u}{\partial r} = 0 \quad \text{at } r = 0 \quad (34)$$

$$u + \frac{k_0}{\mu_0} \frac{\partial \bar{p}}{\partial z} = -\sigma \frac{\partial u}{\partial r} \quad \text{at } r = 1 \quad (35)$$

$$v = 0 \quad \text{at } r = 0 \quad (36)$$

$$v = -\frac{k_0}{\mu_0} \frac{\partial \bar{p}}{\partial r} \quad \text{at } r = 1 \quad (37)$$

$$\frac{\partial \bar{p}}{\partial r} = 0 \quad \text{at } r = 1 + h \quad (38)$$

$$\frac{\partial \bar{p}}{\partial z} = 0 \quad \text{at } z = 0 \quad (39)$$

$$\frac{\partial \bar{p}}{\partial z} = 0 \quad \text{at } z = L \quad (40)$$

$$p = p_A \quad \text{at } z = 0 \quad (41)$$

$$p = p_v \quad \text{at } z = L \quad (42)$$

$$\bar{p} = p \quad \text{at } r = 1 \quad (43)$$

$$\frac{\partial c_1}{\partial r} = 0 \quad \text{at } r = 0 \quad (44)$$

$$\frac{\partial c_2}{\partial r} = 0 \quad \text{at } r = 1 + h \quad (45)$$

$$c_1 = \delta c_2 \quad \text{at } r = 1 \quad (46)$$

$$-D_1 \frac{\partial c_1}{\partial r} = Pe \left(1 - \frac{1}{\delta} \right) \bar{v}_{avg} c_1 - D_2 \frac{\partial c_2}{\partial r} \quad \text{at } r = 1 \quad (47)$$

3. Solution

3.1 Analytical Method and Solution

The solution of the transformed governing Eq. (29) to Eq. (33) using the boundary conditions Eq. (34) to (47) is given as:

Eq. (32) is Laplace's equation in cylindrical coordinates. It is solved for \bar{p} which describes the pressure in tissue region applying the boundary conditions in Eq. (38) to Eq. (40) using the method of separation of variables. We get the value of \bar{p} in terms of A_n which will be obtained using the matching condition at the tissue and capillary interface.

$$\bar{p} = \sum_{n=1}^{\infty} A_n \left[I_0(r\gamma) - \frac{I_1(1+h)\gamma}{K_1(1+h)\gamma} K_0(r\gamma) \right] \sin\left(\frac{n\pi}{l}\right) z \quad (48)$$

where I_0, K_0 and I_1, K_1 represent modified Bessel's function of zeroth order and first order respectively.

The Jeffrey fluid equation for shear stress with varying viscosity including nanoparticle shape parameter given as

$$\tau = \frac{\mu_f(1+A\phi)}{1+\lambda} \{1 + k - kr^m\} \left(-\frac{\partial u}{\partial r}\right) \quad (49)$$

Solving Eq. (30) for finding the value of velocity or u in the capillary region, applying the Jeffrey fluid equation given by Eq. (49) and the boundary condition Eq. (34), we get

$$u = \frac{Re(1+\lambda)}{2\mu_f(1+A\phi)} \frac{\partial p}{\partial z} \left(\frac{r^2}{2} - \frac{r^2 k}{2} + \frac{kr^{m+2}}{m+2}\right) + E_n \quad (50)$$

Now solving Eq. (29) to find the value of pressure in the capillary region or p , applying the boundary conditions Eq. (35) to Eq. (37), Eq. (41) and Eq. (42), we get

$$p = \frac{1}{\left(\frac{1}{6} \frac{k}{6} + \frac{k}{(m+2)(m+4)}\right)} \frac{2(1+A\phi)k_0}{Re(1+\lambda)} \sum_{n=1}^{\infty} A_n \left[\gamma \frac{I_1(1+h)\gamma}{K_1(1+h)\gamma} K_1(\gamma) - \gamma I_1(\gamma) \right] \left(\frac{l^2}{n^2\pi^2}\right) \left(-\sin \frac{n\pi z}{l}\right) - z \frac{(p_A - p_V)}{l} + p_A \quad (51)$$

Using condition in Eq. (43) to find the value of A_n from Eq. (48) and Eq. (51), we get

$$A_n = \frac{\left(\frac{2}{n\pi} \left(\frac{z(p_A - p_V)}{l} - p_A\right) \left(1 - \cos \frac{n\pi}{l}\right) + \frac{2}{n^2\pi^2} (p_A - p_V) \sin \frac{n\pi}{l}\right)}{\left(I_0(r\gamma) - \frac{I_1(1+h)\gamma}{K_1(1+h)\gamma} K_0(r\gamma) + \frac{1}{\left(\frac{1}{6} \frac{k}{6} + \frac{k}{(m+2)(m+4)}\right)} \frac{2(1+A\phi)k_0}{Re(1+\lambda)} \left(\gamma \frac{I_1(1+h)\gamma}{K_1(1+h)\gamma} K_1(\gamma) - \gamma I_1(\gamma)\right)\right)} \quad (52)$$

Using the above value of A_n , the value of $\frac{\partial p}{\partial z}$ will be calculated. Now putting the value of $\frac{\partial p}{\partial z}$ in condition Eq. (35) we get the value of E_n as

$$\begin{aligned}
 E_n = & -\frac{k_0}{\mu_f} \left(\frac{\left(I_0(r\gamma) - \frac{I_1(1+h)\gamma}{K_1(1+h)\gamma} K_0(r\gamma) \sum_{n=1}^{\infty} \frac{2}{n\pi} \left(1 - \cos \frac{n\pi}{l} \right) \left(\frac{P_A - P_V}{l} \right) \sin \frac{n\pi z}{l} \right)}{\left(I_0(r\gamma) - \frac{I_1(1+h)\gamma}{K_1(1+h)\gamma} K_0(r\gamma) + \frac{1}{\left(\frac{1}{6} \frac{k}{6} + (m+2)(m+4) \right)} \frac{2(1+A\phi)k_0}{Re(1+\lambda)} \left(\gamma \frac{I_1(1+h)\gamma}{K_1(1+h)\gamma} K_1(\gamma) - \gamma I_1(\gamma) \right) \right)} + \left(I_0(r\gamma) - \right. \\
 & \left. \frac{I_1(1+h)\gamma}{K_1(1+h)\gamma} K_0(r\gamma) \sum_{n=1}^{\infty} A_n \frac{l}{n\pi} \cos \frac{n\pi z}{l} \right) + \left(1k + \frac{k}{m+2} \right) \frac{Re(1+\lambda)}{2\mu_f(1+A\phi)} \left(\frac{(p_V - p_A)}{l} - \right. \\
 & \left. \frac{\left(\frac{1}{\left(\frac{1}{6} \frac{k}{6} + (m+2)(m+4) \right)} \frac{2(1+A\phi)k_0}{Re(1+\lambda)} \right) \sum_{n=1}^{\infty} \frac{2}{n\pi} \left(1 - \cos \frac{n\pi}{l} \right) \left(\frac{P_A - P_V}{l} \right)}{\left(I_0(r\gamma) - \frac{I_1(1+h)\gamma}{K_1(1+h)\gamma} K_0(r\gamma) + \frac{1}{\left(\frac{1}{6} \frac{k}{6} + (m+2)(m+4) \right)} \frac{2(1+A\phi)k_0}{Re(1+\lambda)} \left(\gamma \frac{I_1(1+h)\gamma}{K_1(1+h)\gamma} K_1(\gamma) - \gamma I_1(\gamma) \right) \right)} \right) \\
 & \left(\frac{1}{\left(\frac{1}{6} \frac{k}{6} + (m+2)(m+4) \right)} \frac{2(1+A\phi)k_0}{Re(1+\lambda)} \right) \sum_{n=1}^{\infty} A_n \frac{l}{n\pi} \cos \frac{n\pi z}{l} - \sigma \frac{Re(1+\lambda)}{2\mu_f(1+A\phi)} \left(\frac{(p_V - p_A)}{l} - \right. \\
 & \left. \frac{\left(\frac{1}{\left(\frac{1}{6} \frac{k}{6} + (m+2)(m+4) \right)} \frac{2(1+A\phi)k_0}{Re(1+\lambda)} \right) \sum_{n=1}^{\infty} \frac{2}{n\pi} \left(1 - \cos \frac{n\pi}{l} \right) \left(\frac{P_A - P_V}{l} \right)}{\left(I_0(r\gamma) - \frac{I_1(1+h)\gamma}{K_1(1+h)\gamma} K_0(r\gamma) + \frac{1}{\left(\frac{1}{6} \frac{k}{6} + (m+2)(m+4) \right)} \frac{2(1+A\phi)k_0}{Re(1+\lambda)} \left(\gamma \frac{I_1(1+h)\gamma}{K_1(1+h)\gamma} K_1(\gamma) - \gamma I_1(\gamma) \right) \right)} \right) \\
 & \left(\frac{1}{\left(\frac{1}{6} \frac{k}{6} + (m+2)(m+4) \right)} \frac{2(1+A\phi)k_0}{Re(1+\lambda)} \right) \sum_{n=1}^{\infty} A_n \frac{l}{n\pi} \cos \frac{n\pi z}{l} \right) \tag{53}
 \end{aligned}$$

The value of \bar{v}_{avg} is calculated as

$$\bar{v}_{avg} = \frac{1}{l} \int_0^l \bar{v} dz \tag{54}$$

we get

$$\begin{aligned}
 \bar{v}_{avg} = & -\frac{k_0}{\mu_f l} \frac{\left(\gamma \frac{I_1(1+h)\gamma}{K_1(1+h)\gamma} K_1(\gamma) - \gamma I_1(\gamma) \right)}{\left(I_0(r\gamma) - \frac{I_1(1+h)\gamma}{K_1(1+h)\gamma} K_0(r\gamma) + \frac{1}{\left(\frac{1}{6} \frac{k}{6} + (m+2)(m+4) \right)} \frac{2(1+A\phi)k_0}{Re(1+\lambda)} \left(\gamma \frac{I_1(1+h)\gamma}{K_1(1+h)\gamma} K_1(\gamma) - \gamma I_1(\gamma) \right) \right)} \left[- \sum_{n=1}^{\infty} \left(2l \left(\frac{p_A - p_V}{l} - p_A \right) \left(1 - \cos \frac{n\pi}{l} \right) + \frac{2}{n\pi} (p_A - \right. \right. \\
 & \left. \left. p_V) \sin \frac{n\pi}{l} \right) \cos \frac{n\pi}{l} + \sum_{n=1}^{\infty} \left(-2lp_A \left(1 - \cos \frac{n\pi}{l} \right) + \frac{2}{n\pi} (p_A - p_V) \sin \frac{n\pi}{l} \right) \right] + \\
 & \frac{\sum_{n=1}^{\infty} \left(\frac{2l^2}{n\pi} \left(\frac{p_A - p_V}{l} \right) \left(1 - \cos \frac{n\pi}{l} \right) \right) \sin \frac{n\pi}{l}}{\left(I_0(r\gamma) - \frac{I_1(1+h)\gamma}{K_1(1+h)\gamma} K_0(r\gamma) + \frac{1}{\left(\frac{1}{6} \frac{k}{6} + (m+2)(m+4) \right)} \frac{2(1+A\phi)k_0}{Re(1+\lambda)} \left(\gamma \frac{I_1(1+h)\gamma}{K_1(1+h)\gamma} K_1(\gamma) - \gamma I_1(\gamma) \right) \right)} \tag{55}
 \end{aligned}$$

Now we have to find the concentration of nanoparticles in the capillary c_1 and the tissue c_2 . We have employed Taylor's dispersion model to solve the diffusion equation. It is assumed that the concentration is symmetrical about the axis of the capillary. The mean radial velocity \bar{v}_{avg} is constant

across l in Eq. (55), therefore the diffusion of nanoparticles is chiefly dependent on the radial variation of c_1 and c_2 . Hence, integrating Eq. (31) while treating $\frac{\partial c_1}{\partial z}$ as constant, and using boundary condition Eq. (44) we get an equation in c_1 and c_2 ; integrating Eq. (33) using boundary condition Eq. (45) to Eq. (47) we get another equation in c_1 and c_2 . Solving both of them simultaneously, we get c_1 and c_2 as

$$c_1 = \frac{Pe}{D_1} \frac{\partial c_1}{\partial z} \left(\frac{Re(1+\lambda)}{2\mu_f(1+A\phi)} \left(-\frac{r^4}{32} + \frac{kr^4}{32} - \frac{kr^{(m+4)}}{(m+2)(m+4)^2} \right) F_n - G_n \frac{r^2}{4} \right) + \frac{m_1}{4D_1} r^2 - \frac{1}{Pe \left(1 - \frac{1}{\delta}\right) \bar{v}_{avg}} \left(\frac{m_2}{2} - \frac{m_2}{2r} (1+h)^3 + \frac{m_1}{D_1} + \frac{1}{D_1} \left(\frac{\partial c_1}{\partial z} \frac{Pe}{D_1} \left(\frac{Re(1+\lambda)}{2\mu_f(1+A\phi)} \left(\frac{1}{8} - \frac{k}{8} + \frac{k(m+3)}{(m+2)(m+4)^2} \right) F_n - \frac{G_n}{2} \right) \right) - \frac{m_1}{4D_1} + \left(\frac{\partial c_1}{\partial z} \frac{Pe}{D_1} \left(\frac{Re(1+\lambda)}{2\mu_f(1+A\phi)} \left(\frac{1}{32} - \frac{k}{32} + \frac{k}{(m+2)(m+4)^2} \right) F_n - \frac{G_n}{4} \right) \right) \right) \quad (56)$$

$$c_2 = -\frac{m_2}{6D_2} r^3 + \frac{m_2(1+h)^3}{D_2} \log r + \frac{m_2}{6D_2} - \frac{m_1}{4\delta D_1} + \frac{1}{\delta} \frac{\partial c_1}{\partial z} \frac{Pe}{D_1} \left(\frac{Re(1+\lambda)}{2\mu_f(1+A\phi)} \left(\frac{1}{32} - \frac{k}{32} + \frac{k}{(m+2)(m+4)^2} \right) F_n - \frac{G_n}{4} \right) - \frac{1}{\delta} \left(\frac{1}{Pe \left(1 - \frac{1}{\delta}\right) \bar{v}_{avg}} \left(\frac{m_2}{2} - \frac{m_2}{2r} (1+h)^3 + \frac{m_1}{D_1} + \frac{1}{D_1} \left(\frac{\partial c_1}{\partial z} \frac{Pe}{D_1} \left(\frac{Re(1+\lambda)}{2\mu_f(1+A\phi)} \left(\frac{1}{8} - \frac{k}{8} + \frac{k(m+3)}{(m+2)(m+4)^2} \right) F_n - \frac{G_n}{2} \right) \right) - \frac{m_1}{4D_1} + \left(\frac{\partial c_1}{\partial z} \frac{Pe}{D_1} \left(\frac{Re(1+\lambda)}{2\mu_f(1+A\phi)} \left(\frac{1}{32} - \frac{k}{32} + \frac{k}{(m+2)(m+4)^2} \right) F_n - \frac{G_n}{4} \right) \right) \right) \right) \quad (57)$$

where

$$F_n = \frac{pV-pA}{l} - \frac{\left(\frac{1}{\left(\frac{1}{6} - \frac{k}{6} + \frac{k}{(m+2)(m+4)}\right)} \frac{2(1+A\phi)k_0}{Re(1+\lambda)} \right) \sum_{n=1}^{\infty} \frac{2}{n\pi} \left(1 - \cos \frac{n\pi}{l}\right) \left(\frac{PA-PV}{l}\right)}{\left(I_0(r\gamma) - \frac{I_1(1+h)\gamma}{K_1(1+h)\gamma} K_0(r\gamma) + \frac{1}{\left(\frac{1}{6} - \frac{k}{6} + \frac{k}{(m+2)(m+4)}\right)} \frac{2(1+A\phi)k_0}{Re(1+\lambda)} \left(\gamma \frac{I_1(1+h)\gamma}{K_1(1+h)\gamma} K_1(\gamma) - \gamma I_1(\gamma) \right) \right)} - \left(\frac{1}{\left(\frac{1}{6} - \frac{k}{6} + \frac{k}{(m+2)(m+4)}\right)} \frac{2(1+A\phi)k_0}{Re(1+\lambda)} \sum_{n=1}^{\infty} A_n \frac{l}{n\pi} \cos \frac{n\pi}{l} Z \right) \quad (58)$$

$$G_n = -\frac{k_0}{\mu_f} \left(\frac{\left(I_0(r\gamma) - \frac{I_1(1+h)\gamma}{K_1(1+h)\gamma} K_0(r\gamma) \right) \sum_{n=1}^{\infty} \frac{2}{n\pi} \left(1 - \cos \frac{n\pi}{l}\right) \frac{PA-PV}{l} \sin \frac{n\pi}{l} z}{\left(I_0(r\gamma) - \frac{I_1(1+h)\gamma}{K_1(1+h)\gamma} K_0(r\gamma) + \frac{1}{\left(\frac{1}{6} - \frac{k}{6} + \frac{k}{(m+2)(m+4)}\right)} \frac{2(1+A\phi)k_0}{Re(1+\lambda)} \left(\gamma \frac{I_1(1+h)\gamma}{K_1(1+h)\gamma} K_1(\gamma) - \gamma I_1(\gamma) \right) \right)} + \left(I_0(r\gamma) - \frac{I_1(1+h)\gamma}{K_1(1+h)\gamma} K_0(r\gamma) \right) \sum_{n=1}^{\infty} A_n \frac{l}{n\pi} \cos \frac{n\pi}{l} z - \left(1 - k + \frac{k}{m+2} \right) \frac{Re(1+\lambda)}{2\mu_f(1+A\phi)} a_2 - \sigma \frac{Re(1+\lambda)}{2\mu_f(1+A\phi)} a_2 \quad (59)$$

3.2 Finite Difference Method

The current problem was also solved using finite difference scheme for solving coupled partial differential equation [31] using MATLAB. The finite difference equations and boundary conditions are stated below:

$$\frac{u_{m+1}-u_m}{2(z_{m+1}-z_m)} + \frac{v_n}{r_n} + \frac{v_{m+1}-v_m}{2(z_{m+1}-z_m)} = 0 \quad (60)$$

$$\frac{p_{m+1}-p_m}{2(z_{m+1}-z_m)} = -\frac{1}{Re} \frac{1}{r_{n+1}-r_n} \frac{1}{2(r_{n+1}-r_n)} (\tau_{n+1}r_{n+1} - \tau_n r_n) \quad (61)$$

$$Pe(u_n) \left(\frac{c_{1,n+1} - c_{1,n}}{2(z_{m+1} - z_m)} \right) = D_1 \left(\frac{c_{1,n-1} - 2c_{1,n} + c_{1,n+1}}{(r_{n+1} - r_n)^2} + \frac{1}{r_{n+1} - r_n} \frac{c_{1,n+1} - c_{1,n}}{2(r_{n+1} - r_n)} \right) + m_1 \quad (62)$$

$$\nabla_{n,m}^2 \overline{p_{n,m}} = 0 \quad (63)$$

$$0 = D_2 \left(\frac{c_{2,n-1} - 2c_{2,n} + c_{2,n+1}}{(r_{n+1} - r_n)^2} + \frac{1}{r_{n+1} - r_n} \frac{c_{2,n+1} - c_{2,n}}{2(r_{n+1} - r_n)} \right) + m_2 \quad (64)$$

$$\frac{u_2 - u_1}{2(r_2 - r_1)} = 0 \quad \text{at } r_1 = 0 \quad (65)$$

$$u_1 + \frac{k_0}{\mu_0} \frac{\overline{p_{m+1}} - \overline{p_m}}{2(z_{m+1} - z_m)} = -\sigma \frac{v_2 - v_1}{2(r_2 - r_1)} \quad \text{at } r_1 = 0 \quad (66)$$

$$v_1 = 0 \quad \text{at } r_1 = 0 \quad (67)$$

$$v_n = -\frac{k_0}{\mu_0} \frac{\overline{p_{n+1}} - \overline{p_n}}{2(r_{n+1} - r_n)} \quad \text{at } r_n = n \quad (68)$$

$$\frac{\overline{p_{n+1}} - \overline{p_n}}{2(r_{n+1} - r_n)} = 0 \quad \text{at } r_n = n + h \quad (69)$$

$$\frac{\overline{p_2} - \overline{p_1}}{2(z_2 - z_1)} = 0 \quad \text{at } z_1 = 0 \quad (70)$$

$$\frac{\overline{p_{m+1}} - \overline{p_m}}{2(z_{m+1} - z_m)} = 0 \quad \text{at } z_m = L \quad (71)$$

$$p_1 = p_A \quad \text{at } z_1 = 0 \quad (72)$$

$$p_m = p_v \quad \text{at } z_m = L \quad (73)$$

$$\overline{p_n} = p_n \quad \text{at } r_n = n \quad (74)$$

$$\frac{c_{1,2} - c_{1,1}}{2(r_2 - r_1)} = 0 \quad \text{at } r_1 = 0 \quad (75)$$

$$\frac{c_{2,n+1} - c_{2,n}}{2(r_{n+1} - r_n)} = 0 \quad \text{at } r_n = n + h \quad (76)$$

$$c_{1,n} = \delta c_{2,n} \quad \text{at } r_n = n \quad (77)$$

$$-D_1 \frac{c_{1,n+1} - c_{1,n}}{2(r_{n+1} - r_n)} = Pe \left(1 - \frac{1}{\delta} \right) \overline{v}_{avg} c_{1,n} - D_2 \frac{c_{2,n+1} - c_{2,n}}{2(r_{n+1} - r_n)} \quad \text{at } r_n = n \quad (78)$$

The algorithm for solving the equations is given as:

- I. The radial domain is represented by a mesh of (n+1) grid points $0 = r_0 < r_1 < r_2 < \dots < r_{n-1} < r_n = 1$.
- II. We seek the solution of u , c_1 and c_2 at the mesh points for their respective regions.
- III. The difference Eq. (60) to Eq. (64) and boundary conditions Eq. (65) to Eq. (78) are used to obtain the values at each grid point applying Thomas algorithm for tridiagonal system of matrices.

Table 2 below compares the analytical and numerical values of nanofluid velocity in the capillary region and nanoparticle concentrations in the capillary and tissue region respectively.

Table 2

Comparison of the analytical and numerical values of nanofluid velocity in the capillary region and nanoparticle concentrations in the capillary and tissue region
 $A=1.9, \phi=0.01, \lambda=2.0, k=0.2, m=0.2$

r	u (analytical)	u (FDM)	c_1 (analytical)	c_1 (FDM)	c_2 (analytical)	c_2 (FDM)
0.0	1.000000	1.000000	3.000000	3.000000	-	-
0.2	0.973920	0.973916	2.923761	2.923756	-	-
0.4	0.894162	0.894159	2.680182	2.680175	-	-
0.6	0.755945	0.755940	2.224670	2.224662	-	-
0.8	0.551593	0.551587	1.482907	1.482900	-	-
1.0	0.270171	0.270168	0.103251	0.103246	0.103251	0.103246
1.2	-	-	-	-	0.103228	0.103224
1.4	-	-	-	-	0.103208	0.103205
1.6	-	-	-	-	0.103193	0.103187
1.8	-	-	-	-	0.103180	0.103173
2.0	-	-	-	-	0.103169	0.103165

Meanwhile Table 3 below gives the error analysis.

Table 3

Error analysis

$A=1.9, \phi=0.01, \lambda=2.0, k=0.2, m=0.2$

r	u	c_1	c_2
0.0	0.000000	0.000000	-
0.2	0.000004	0.000005	-
0.4	0.000003	0.000007	-
0.6	0.000005	0.000008	-
0.8	0.000006	0.000007	-
1.0	0.000003	0.000005	0.000005
1.2	-	-	0.000004
1.4	-	-	0.000003
1.6	-	-	0.000006
1.8	-	-	0.000007
2.0	-	-	0.000004

4. Graphical Results and Discussions

This section explains the graphical effect of relevant parameters on the profiles of velocity and concentration against radial direction. The observations are made on for different values of shape parameter of nanoparticles (A), volume fraction of nanoparticles (ϕ), Jeffrey fluid parameter (λ), viscosity parameter (k) and viscosity index (m). Figure 2 until Figure 6 represent the graphs of velocity in capillary region against radial direction followed by Figure 7 until Figure 11 that represent the graphs of concentration of nanoparticles in capillary and tissue region against radial direction.

Figure 2 depicts velocity of nanofluid in capillary region against radial direction (r) for different values of shape parameter (A). It can be seen that lesser the value of shape parameter, greater is the axial velocity. Consequently, bricks that have least value of shape parameter, show greatest velocity. The consequence of the shape of nanoparticles on the velocity is because of the viscosity dependence on the shape parameter. Blades and cylinders have almost same viscosity in nanofluid due to elongated structures, thus they show overlapping profile for velocity. Similar results were given by

Madhura *et al.*, [23]. Lee *et al.*, [24], in their experimental study of nanoparticle diffusion through biological barriers like tissues, reported that rod-shaped nanoparticles had greater velocity than spherical shaped nanoparticles while diffusing. Thus, platelet shaped nanoparticles show least rise in velocity while brick shaped nanoparticles have maximum rise in velocity. Similar results were reported by Timofeeva *et al.*, [25].

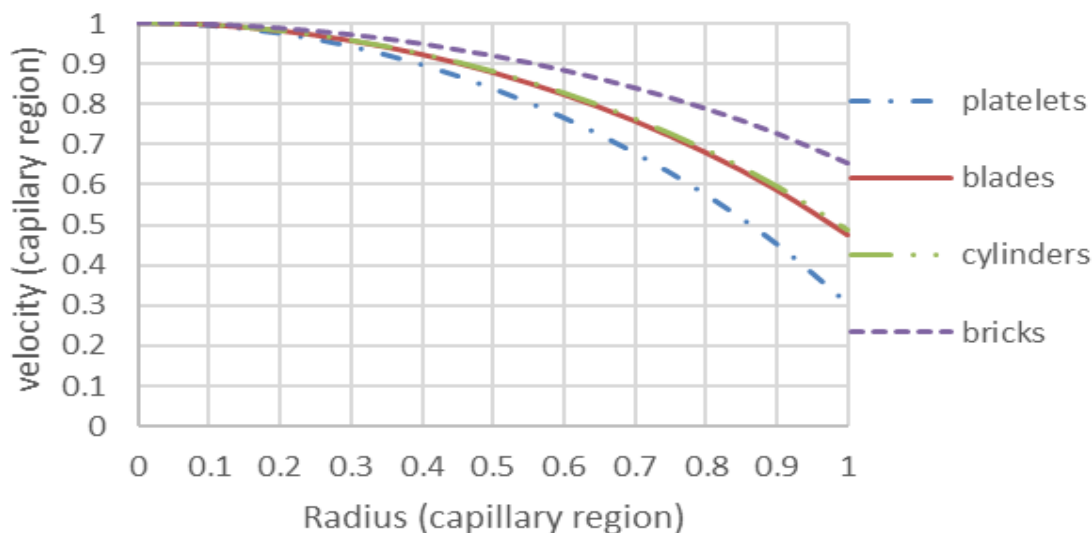


Fig. 2. Variation of velocity with radius for different shape parameter A of nanoparticles

Figure 3 shows velocity in capillary region against radial direction (r) for different values of volume fraction (ϕ) for brick shaped nanoparticles. The trend shows that the increase in the value of volume fraction of nanoparticles causes a decrease in the velocity of nanoparticles. This is so because as the volume fraction increases, the number of nanoparticles in the blood increases, which makes the nanofluid more viscous. Identical observations were given by Timofeeva *et al.*, [25] in their experimental study. The enhancement in viscosity causes an enhancement in the friction force which causes a reduction in velocity. Thus, velocity increases with the decrease in the volume fraction. Similar observations were made by Ijaz and Nadeem [26].

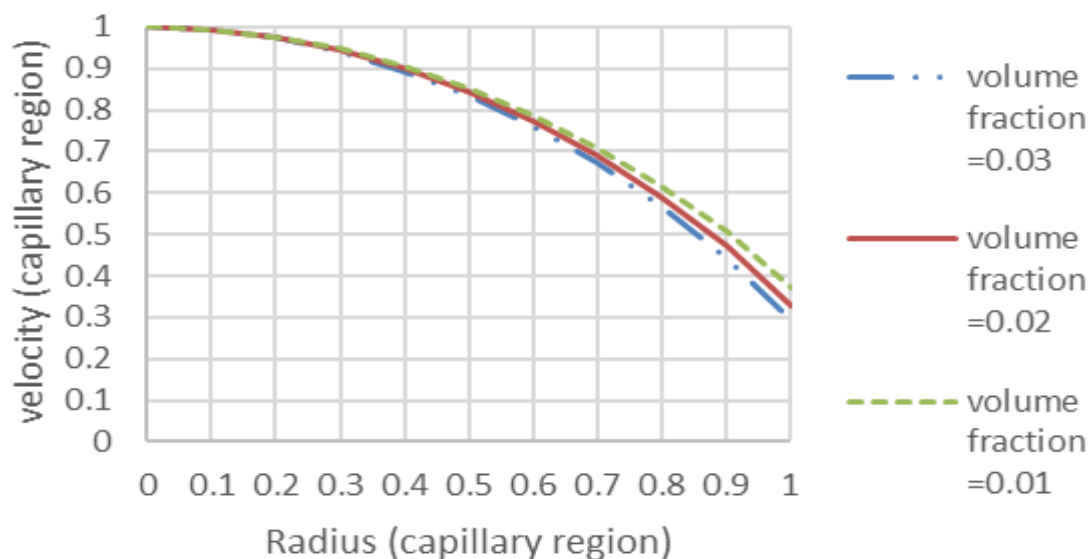


Fig. 3. Variation of velocity with radius for different values of volume fraction ϕ of nanoparticles

Figure 4 shows velocity in capillary region against radial direction (r) for different values of Jeffrey parameter (λ) for brick shaped nanoparticles. The graph shows that larger the value of Jeffrey parameter, larger the velocity. Jeffrey parameter represents the ratio of relaxation to retardation time. Also, Jeffrey fluid show shear-thinning properties. Rise in Jeffrey parameter causes an increase in convection coefficient at a given temperature [2], which in turn increases the movement of nanoparticles in nanofluid, thus increasing their velocity.

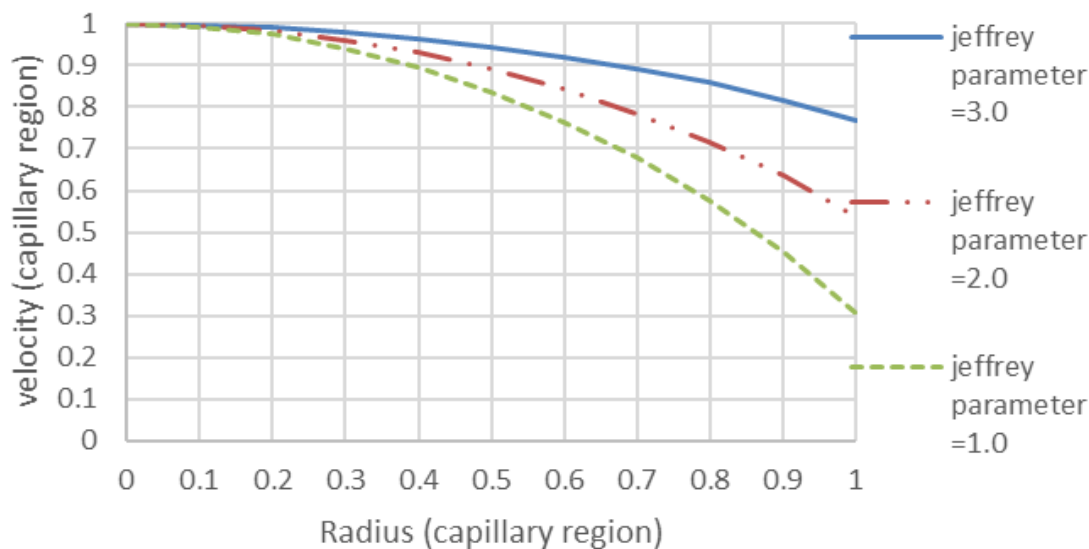


Fig. 4. Variation of velocity with radius for different values of Jeffrey parameter λ

Figure 5 shows velocity in capillary region against radial direction (r) for different values of viscosity parameter (k) for brick shaped nanoparticles. The trend depicts that the velocity increases for increasing values of viscosity parameter. Viscosity parameter exhibits the behaviour of shear thinning fluids. As its value increases, the viscosity decreases and thus the velocity increases.

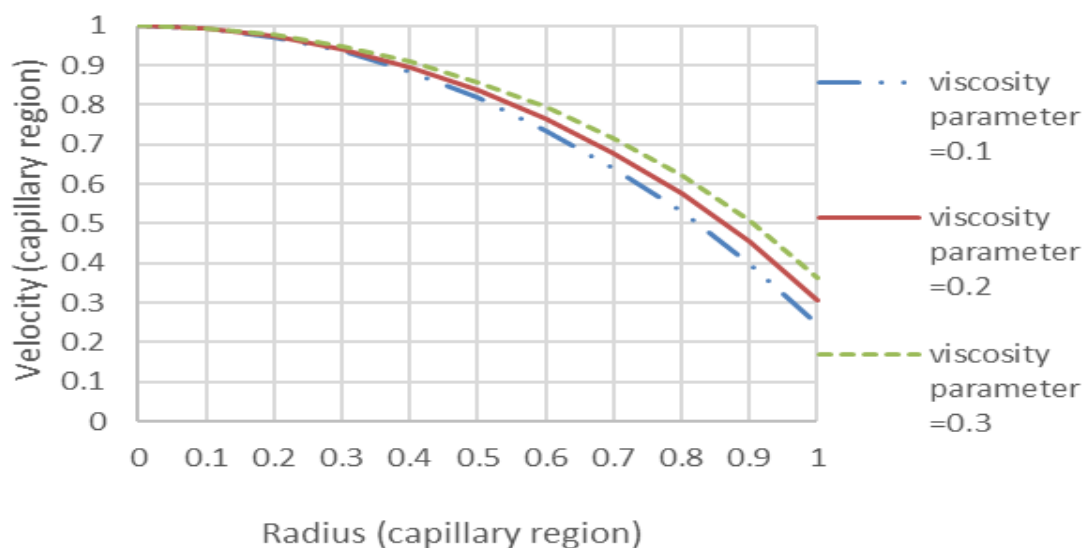


Fig. 5. Variation of velocity against radius for different values of viscosity parameter k

Figure 6 describes velocity in capillary region against radial direction (r) for different values of viscosity index (m) for brick shaped nanoparticles. The trend shows that greater the value of viscosity

index, greater the velocity of the nanofluid. The viscosity index is a measure of the constancy of the viscosity. The greater the viscosity index, lesser is viscosity affected by changes in temperature. This implies that at a given temperature, greater the viscosity index, lesser the viscosity and in turn, greater is the velocity of nanofluid.

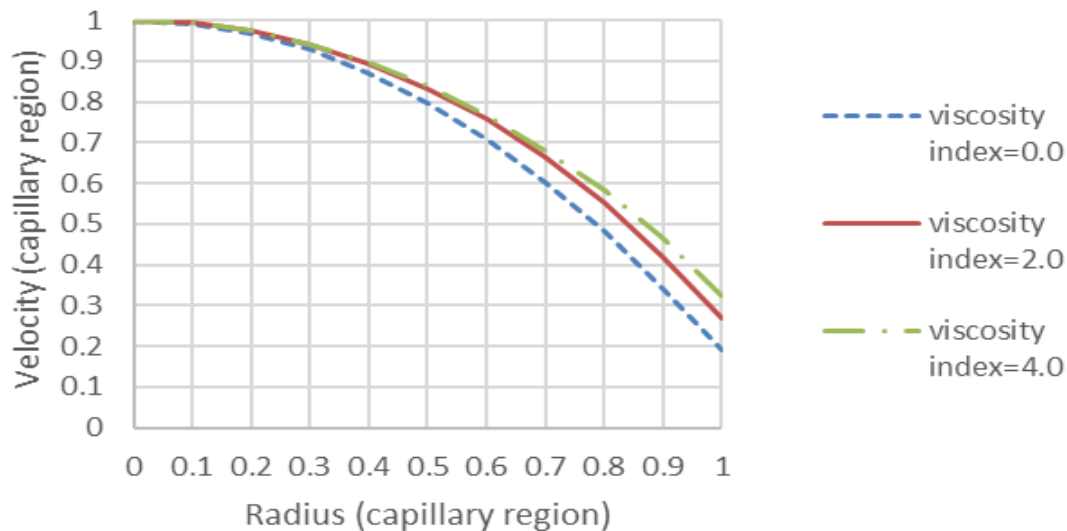
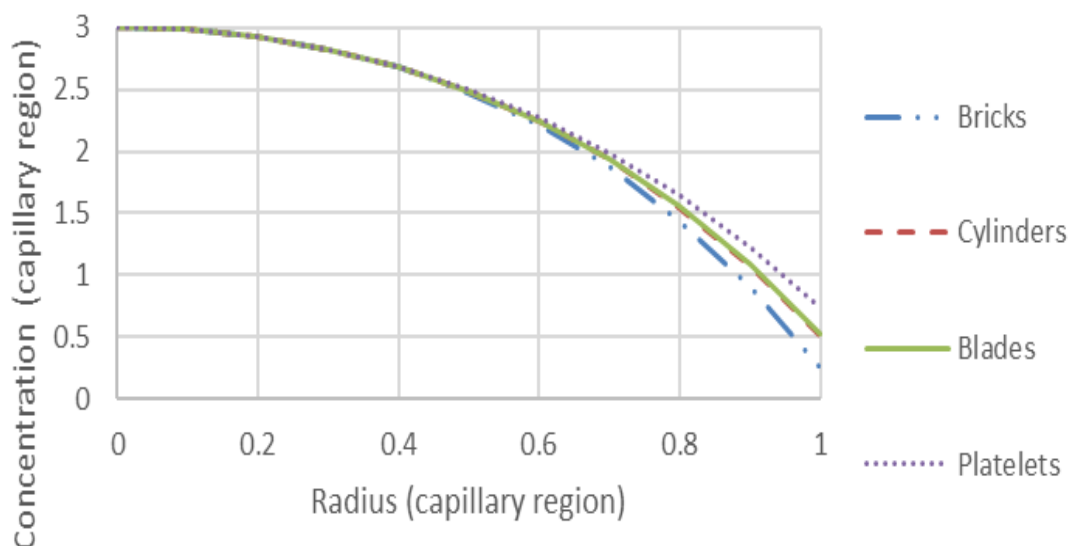
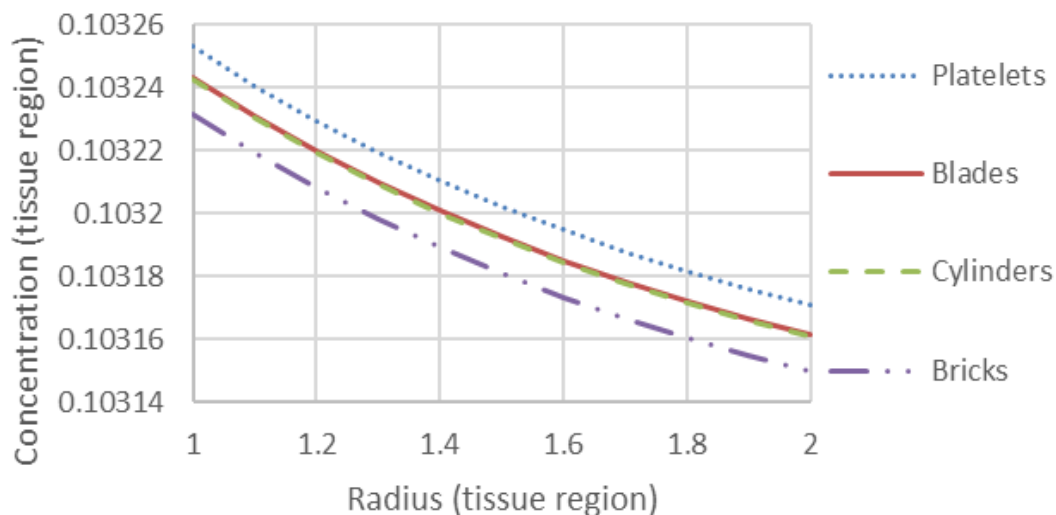


Fig. 6. Variation of velocity against radius for different values of viscosity index m

Figures 7(a) and Figure 7(b) show concentration against radial direction (r) for different values of shape parameter (A) in capillary region and tissue region respectively. The trend shows that higher the value of shape parameter, greater the concentration. Thus, platelets show maximum rise in concentration and bricks show minimum rise in concentration. The high value of shape parameter depicts higher diffusion rates, thus higher concentrations. Results obtained are in accordance with the experimental results obtained by Lee *et al.*, [24].



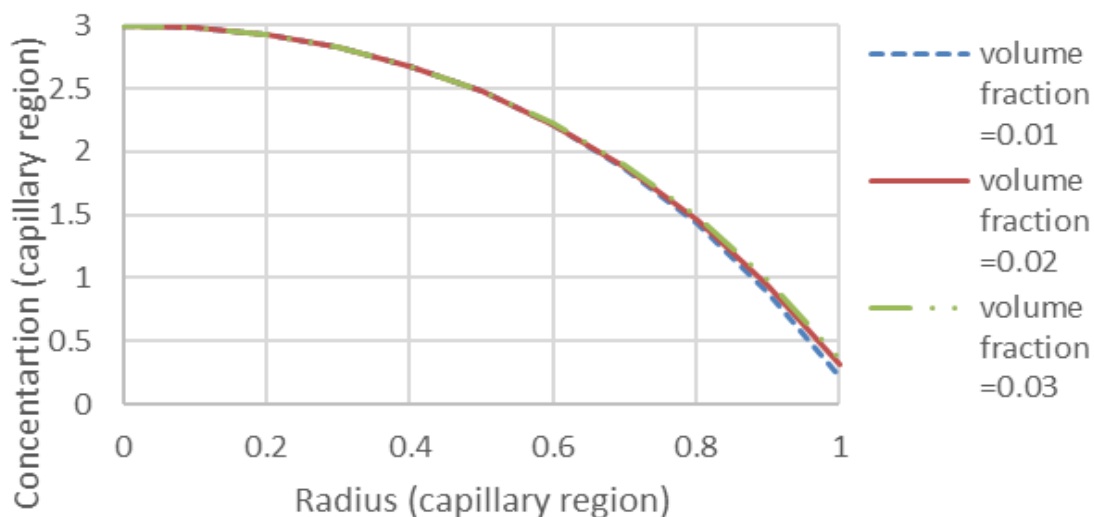
(a)



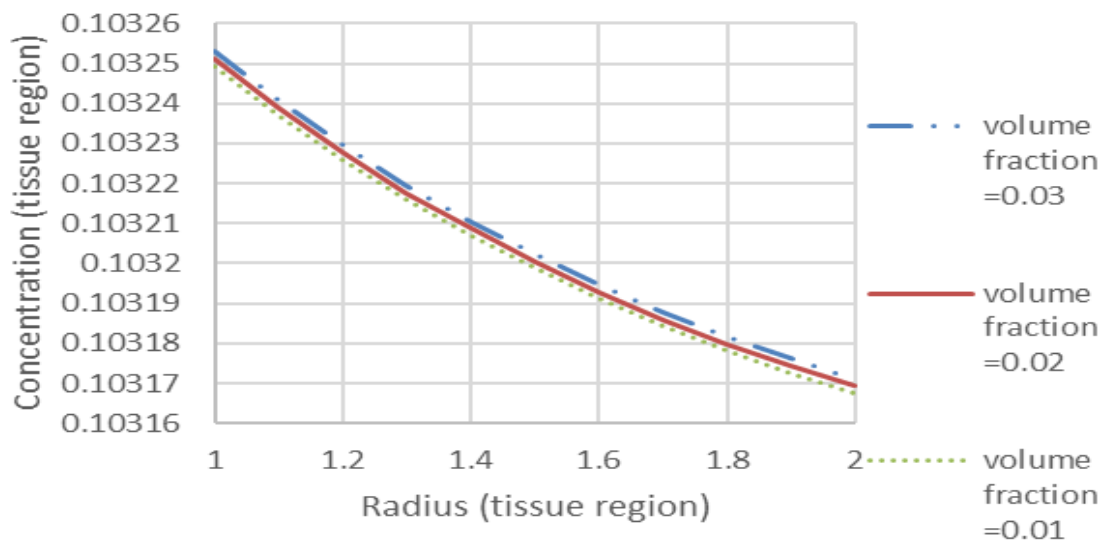
(b)

Fig. 7. Variation of concentration with radius for different shape parameter A of nanoparticles in (a) Capillary region (b) Tissue region

Figures 8(a) and Figure 8(b) display concentration against radial direction (r) for different values of volume fraction (ϕ) in the capillary region and tissue region respectively for brick shaped nanoparticles. The trend depicts that higher the value of volume fraction, greater the concentration. Volume fraction represents value of volume of nanoparticles divided by the volume of all constituents of the nanofluid. Thus, increasing the volume fraction, increases the number of nanoparticles, which increases the concentration of nanoparticles. Analogous observations were given by Timofeeva *et al.*, [25] in their experimental study.



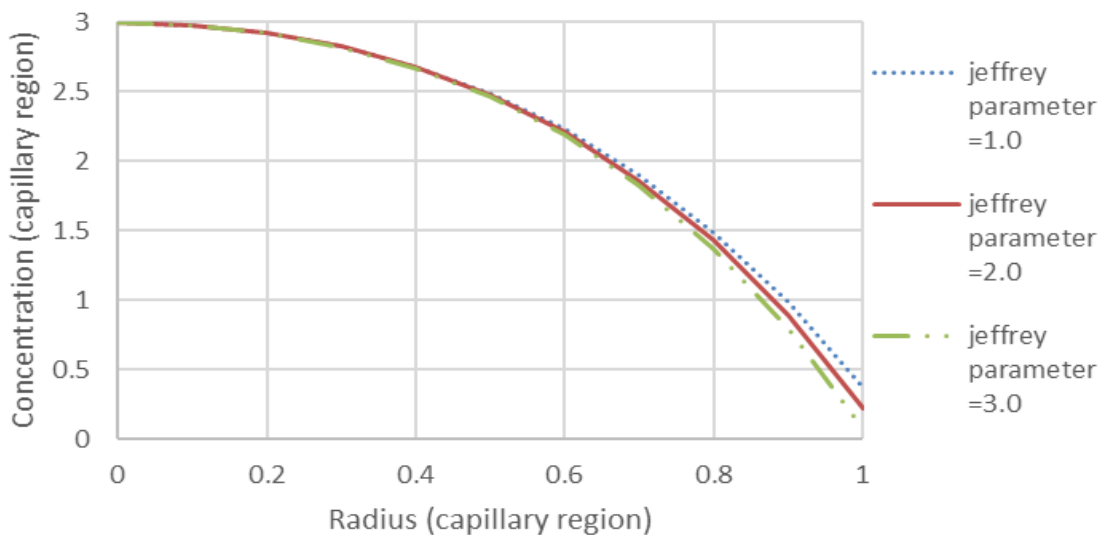
(a)



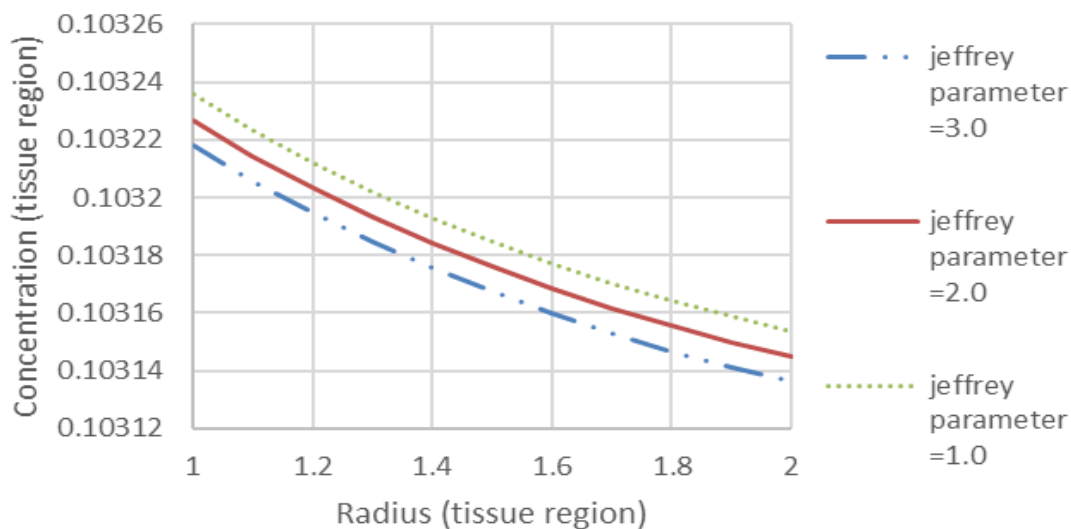
(b)

Fig. 8. Variation of concentration with radius for different values of volume fraction ϕ of nanoparticles in (a) Capillary region (b) Tissue region

Figures 9(a) and Figure 9(b) show concentration against radial direction (r) for different values of Jeffrey parameter (λ) in the capillary region and tissue region respectively for brick shaped nanoparticles. The profiles depict decrease in concentration as the value of Jeffrey parameter increases. Since Jeffrey parameter represents the relaxation to retardation time, increase in its value will increase the convection which will lead increase in axial dispersion or axial velocity. Jeffrey fluids possess shear-thinning properties too. This will accredit to decay in concentration due to decrease in viscosity. Parallel results were obtained by Chauhan and Tiwari [2].



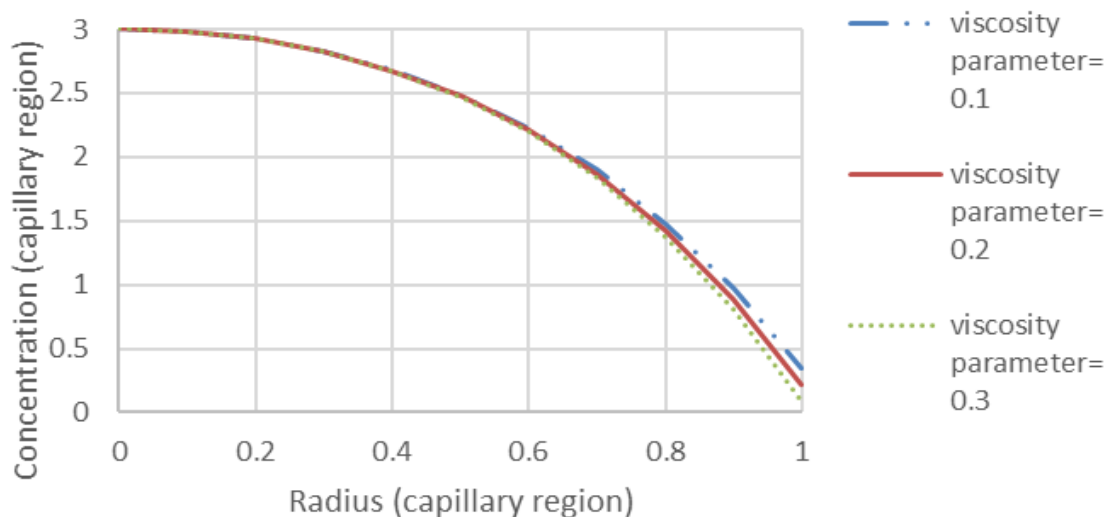
(a)



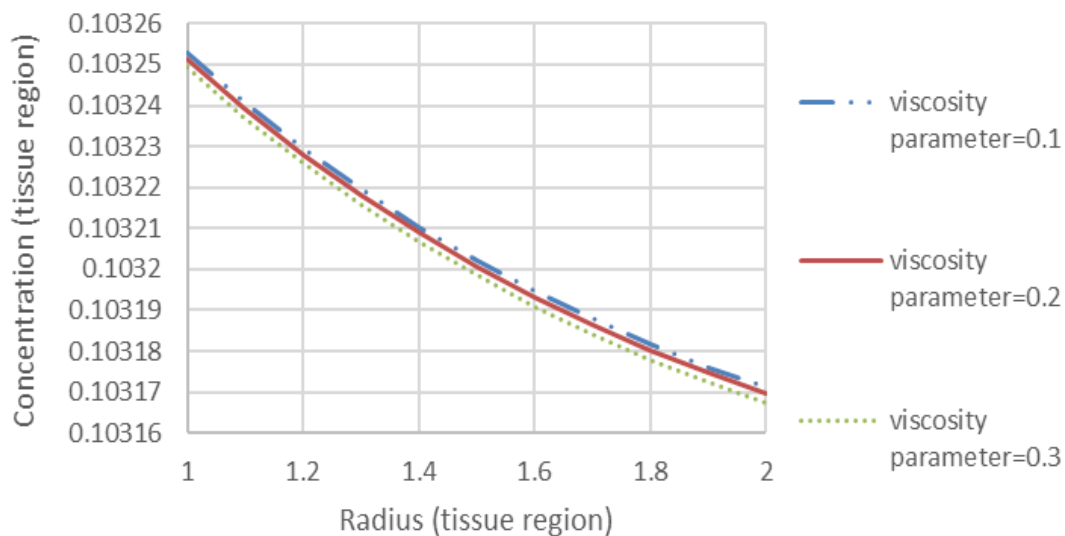
(b)

Fig. 9. Variation of concentration with radius for different values of Jeffrey parameter λ in (a) Capillary region (b) Tissue region

Figure 10(a) and Figure 10(b) display concentration against radial direction (r) for different values of viscosity parameter (k) in the capillary region and tissue region respectively for brick shaped nanoparticles. The graphs show that increase in the value of viscosity parameter causes a decrease in concentration. Increase in the value of viscosity parameter increases the velocity which reduces the concentration due to decreasing viscosity [2]. So, reduction in viscosity parameter reduces the axial dispersion and hence increases the concentration.



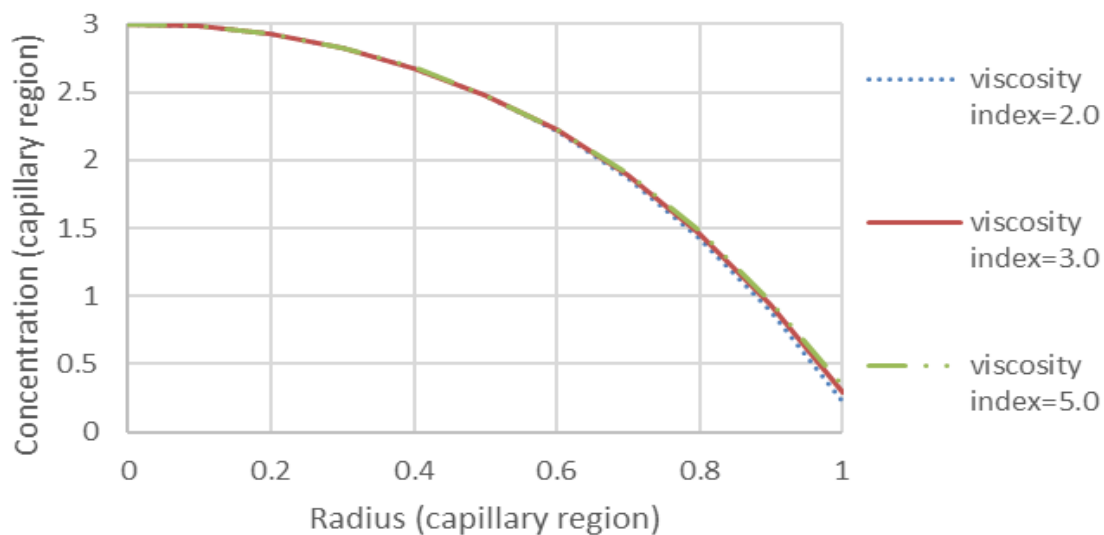
(a)



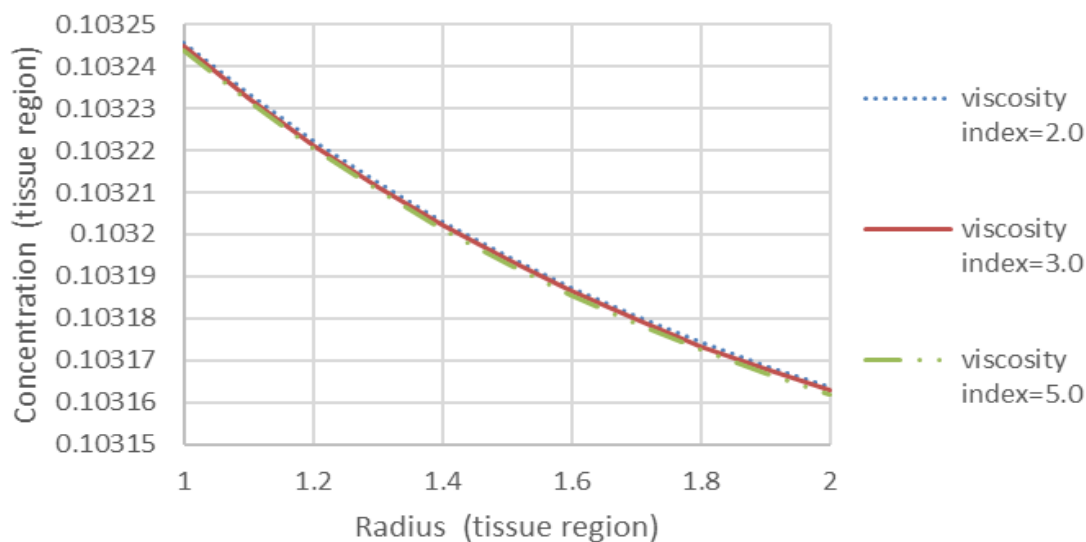
(b)

Fig. 10. Variation of concentration with radius for different values of viscosity parameter k in (a) Capillary region (b) Tissue region

Figure 11(a) and Figure 11(b) show concentration against radial direction (r) for different values of viscosity index (m) in the capillary region and tissue region respectively for brick shaped nanoparticles. The trend shows that with the increase in the value of viscosity index, the concentration decreases. The increase in the value of viscosity index causes an increase in the velocity that decreases the axial dispersion which in turn decreases the concentration. This is because the time taken in diffusion process increases due to the increase in viscosity index [2].



(a)



(b)

Fig. 11. Variation of concentration against radius for different values of viscosity index m in (a) Capillary region (b) Tissue region

5. Conclusion

Nanoparticles have evinced as having befitting therapeutic applications for treating blockages in vasculature or killing diseased cells through agent-based approach or their direct usage as drugs. The diffusivity of nanoparticles is affected by shape of nanoparticle and the type of base fluid in which they are diffused. By present model we have analysed the effects of diffusion of nanoparticles in the capillary-tissue exchange system. Analytical expressions for velocity and concentration were derived. Efforts were also made to compare the results with the solution obtained using finite difference method. The effects of shape parameter of nanoparticles (A), volume fraction of nanoparticles (ϕ), Jeffrey fluid parameter (λ), viscosity parameter (k) and viscosity index (m) on velocity and concentration of the nanoparticles were investigated. Major findings of the study are summarized as follows:

- I. The velocity decreases with the increase in the values of shape parameter and volume fraction.
- II. The maximum velocity is observed for brick shaped nanoparticles and minimum is observed for platelets.
- III. The velocity increases with the increase in the values of Jeffrey parameter, viscosity parameter and viscosity index.
- IV. The concentration increases with the increase in the value of shape parameter and volume fraction.
- V. The maximum concentration is observed for platelets and minimum is observed for bricks.
- VI. The concentration decreases with the increase in the values of Jeffrey parameter, viscosity parameter and viscosity index.

For the therapeutic treatment involving the diffusion of nano-drugs in the circulatory system, the study of concentration of nanoparticles in the capillary-tissue exchange system is highly significant so that its therapeutic and toxic effects can be controlled accordingly. Also, the above model can be further developed for regulating nanoparticle clustering as they interact with the components of blood.

Acknowledgement

This research did not receive any specific grant from funding agencies in the public, commercial, or not-for-profit sectors.

References

- [1] Qiu, Xianjie. *Fluid flow in a Krogh cylinder: A model for a single capillary and surrounding tissue*. Missouri University of Science and Technology, 2018.
- [2] Chauhan, Satyendra Singh, and Ashish Tiwari. "Solute dispersion in non-Newtonian fluids flow through small blood vessels: A varying viscosity approach." *European Journal of Mechanics-B/Fluids* 94 (2022): 200-211. <https://doi.org/10.1016/j.euromechflu.2022.02.009>
- [3] Tandon, P. N., and R. Agarwal. "A study of diffusion is modelled in normal and stenotic capillary tissue exchange system." In *Proc. Int. Conf. on Computational Methods in Flow Analysis*, vol. 2, p. 1154. 1988.
- [4] Bali, Rekha, Bhawini Prasad, and Swati Mishra. "A Review on Mathematical Models for Nanoparticle Delivery in the Blood." *International Journal of Advanced Research* 10, no. 04 (2022): 130–46. <https://doi.org/10.21474/IJAR01/14526>
- [5] Qiu, Lin, Ning Zhu, Yanhui Feng, Efstathios E. Michaelides, Gawel Żyła, Dengwei Jing, Xinxin Zhang, Pamela M. Norris, Christos N. Markides, and Omid Mahian. "A review of recent advances in thermophysical properties at the nanoscale: From solid state to colloids." *Physics Reports* 843 (2020): 1-81. <https://doi.org/10.1016/j.physrep.2019.12.001>
- [6] Simpson, Sarah, Austin Schelfhout, Chris Golden, and Saeid Vafaei. "Nanofluid thermal conductivity and effective parameters." *Applied Sciences* 9, no. 1 (2018): 87. <https://doi.org/10.3390/app9010087>
- [7] Deng, Yudi, Xudong Zhang, Haibin Shen, Qiangnan He, Zijian Wu, Wenzhen Liao, and Miaomiao Yuan. "Application of the nano-drug delivery system in treatment of cardiovascular diseases." *Frontiers in bioengineering and biotechnology* 7 (2020): 489. <https://doi.org/10.3389/fbioe.2019.00489>
- [8] Kwatra, S. "Nanotechnology and medicine—The upside and the downside." *IJDDR* 5 (2013): 0975-9344.
- [9] Gonçalves, Inês, Reinaldo Souza, Gonçalo Coutinho, João Miranda, Ana Moita, José Eduardo Pereira, António Moreira, and Rui Lima. "Thermal conductivity of nanofluids: a review on prediction models, controversies and challenges." *Applied Sciences* 11, no. 6 (2021): 2525. <https://doi.org/10.3390/app11062525>
- [10] Moghaddam, Hossein Asadi, Ashkan Ghafouri, and Reza Faridi Khouzestani. "Viscosity and thermal conductivity correlations for various nanofluids based on different temperature and nanoparticle diameter." *Journal of the Brazilian Society of Mechanical Sciences and Engineering* 43, no. 6 (2021): 303. <https://doi.org/10.1007/s40430-021-03017-1>
- [11] Ellahi, R., S. U. Rahman, and S. Nadeem. "Blood flow of Jeffrey fluid in a catheterized tapered artery with the suspension of nanoparticles." *Physics Letters A* 378, no. 40 (2014): 2973-2980. <https://doi.org/10.1016/j.physleta.2014.08.002>
- [12] Rahman, S. U., R. Ellahi, Sohail Nadeem, and QM Zaigham Zia. "Simultaneous effects of nanoparticles and slip on Jeffrey fluid through tapered artery with mild stenosis." *Journal of Molecular liquids* 218 (2016): 484-493. <https://doi.org/10.1016/j.molliq.2016.02.080>
- [13] Krogh, August. "The number and distribution of capillaries in muscles with calculations of the oxygen pressure head necessary for supplying the tissue." *The Journal of physiology* 52, no. 6 (1919): 409-415. <https://doi.org/10.1113/jphysiol.1919.sp001839>
- [14] Popel, Aleksander S. "Analysis of capillary-tissue diffusion in multicapillary systems." *Mathematical biosciences* 39, no. 3-4 (1978): 187-211. [https://doi.org/10.1016/0025-5564\(78\)90053-6](https://doi.org/10.1016/0025-5564(78)90053-6)
- [15] Blum, Jacob J. "Concentration profiles in and around capillaries." *American Journal of Physiology-Legacy Content* 198, no. 5 (1960): 991-998. <https://doi.org/10.1152/ajplegacy.1960.198.5.991>
- [16] Levitt, David G. "Theoretical model of capillary exchange incorporating interactions between capillaries." *American Journal of Physiology-Legacy Content* 220, no. 1 (1971): 250-255. <https://doi.org/10.1152/ajplegacy.1971.220.1.250>
- [17] Tandon, P. N., J. K. Misra, and R. L. Verma. "Peripheral-layer viscosity and microstructural effects on the capillary-tissue fluid exchange." *Mathematical Biosciences* 62, no. 1 (1982): 7-22. [https://doi.org/10.1016/0025-5564\(82\)90060-8](https://doi.org/10.1016/0025-5564(82)90060-8)
- [18] Siddiqui, S. U., and Shailesh Mishra. "A study of modified Casson's fluid in modelled normal and stenotic capillary-tissue diffusion phenomena." *Applied mathematics and computation* 189, no. 2 (2007): 1048-1057. <https://doi.org/10.1016/j.amc.2006.11.151>

- [19] Singh, Sapna. "Numerical modeling for the modified power law fluid in stenotic capillary-tissue diffusion phenomena." *Archives of Applied Science Research* 2, no. 1 (2010): 106.
- [20] Bali, Rekha, Swati Mishra, and Mamta Mishra. "Effect of Deformation of Red Cell on Nutritional Transport in Capillary-Tissue Exchange System." *Applied Mathematics* 2, no. 11 (2011): 1417-1423. <https://doi.org/10.4236/am.2011.211200>
- [21] Ismaeel, A. M., M. A. Mansour, F. S. Ibrahim, and F. M. Hady. "Numerical simulation for nanofluid extravasation from a vertical segment of a cylindrical vessel into the surrounding tissue at the microscale." *Applied Mathematics and Computation* 417 (2022): 126758. <https://doi.org/10.1016/j.amc.2021.126758>
- [22] Mun, Ellina A., Claire Hannell, Sarah E. Rogers, Patrick Hole, Adrian C. Williams, and Vitaliy V. Khutoryanskiy. "On the role of specific interactions in the diffusion of nanoparticles in aqueous polymer solutions." *Langmuir* 30, no. 1 (2014): 308-317. <https://doi.org/10.1021/la4029035>
- [23] Madhura, K. R., Babitha Atiwali, and S. S. Iyengar. "Influence of nanoparticle shapes on natural convection flow with heat and mass transfer rates of nanofluids with fractional derivative." *Mathematical Methods in the Applied Sciences* (2021). <https://doi.org/10.1002/mma.7404>
- [24] Lee, Benjamin J., Yahya Cheema, Shahed Bader, and Gregg A. Duncan. "Shaping nanoparticle diffusion through biological barriers to drug delivery." *JCIS Open* 4 (2021): 100025. <https://doi.org/10.1016/j.jciso.2021.100025>
- [25] Timofeeva, Elena V., Jules L. Routbort, and Dileep Singh. "Particle shape effects on thermophysical properties of alumina nanofluids." *Journal of applied physics* 106, no. 1 (2009): 014304. <https://doi.org/10.1063/1.3155999>
- [26] Ijaz, S., and S. Nadeem. "Examination of nanoparticles as a drug carrier on blood flow through catheterized composite stenosed artery with permeable walls." *Computer methods and programs in biomedicine* 133 (2016): 83-94. <https://doi.org/10.1016/j.cmpb.2016.05.004>
- [27] Ali, Farhad, Saqib Murtaza, Ilyas Khan, Nadeem Ahmad Sheikh, and Kottakkaran Sooppy Nisar. "Atangana–Baleanu fractional model for the flow of Jeffrey nanofluid with diffusion-thermo effects: applications in engine oil." *Advances in Difference Equations* 2019, no. 1 (2019): 1-21. <https://doi.org/10.1186/s13662-019-2222-1>
- [28] Kotnurkar, Asha S., and Vijaylaxmi T. Talawar. "Influence of Jeffrey nanofluid on peristaltic motion in an inclined endoscope." *Computational Engineering and Physical Modeling* 4, no. 2 (2021): 68-94.
- [29] Hayat, Tasawar, Sajid Qayyum, and Ahmed Alsaedi. "Mechanisms of nonlinear convective flow of Jeffrey nanofluid due to nonlinear radially stretching sheet with convective conditions and magnetic field." *Results in physics* 7 (2017): 2341-2351. <https://doi.org/10.1016/j.rinp.2017.06.052>
- [30] Shahzad, Faisal, Dumitru Baleanu, Wasim Jamshed, Kottakkaran Sooppy Nisar, Mohamed R. Eid, Rabia Safdar, and Khadiga Ahmed Ismail. "Flow and heat transport phenomenon for dynamics of Jeffrey nanofluid past stretchable sheet subject to Lorentz force and dissipation effects." *Scientific Reports* 11, no. 1 (2021): 22924. <https://doi.org/10.1038/s41598-021-02212-3>
- [31] Nguyen, T. V., and Ralph E. White. "A finite difference procedure for solving coupled, nonlinear elliptic partial differential equations." *Computers & chemical engineering* 11, no. 5 (1987): 543-546. [https://doi.org/10.1016/0098-1354\(87\)80029-7](https://doi.org/10.1016/0098-1354(87)80029-7)
- [32] Barua, Sutapa, and Samir Mitragotri. "Challenges associated with penetration of nanoparticles across cell and tissue barriers: a review of current status and future prospects." *Nano today* 9, no. 2 (2014): 223-243. <https://doi.org/10.1016/j.nantod.2014.04.008>
- [33] Ramana Reddy, J. V., and D. Srikanth. "Impact of blood vessel wall flexibility on the temperature and concentration dispersion." *Journal of Applied and Computational Mechanics* 6, no. 3 (2020): 564-581.
- [34] Tan, Jian Hong, Toru Yamada, Yutaka Asako, Lit Ken Tan, and Nor Azwadi Che Sidik. "Study of Self Diffusion of Nanoparticle Using Dissipative Particle Dynamics." *Journal of Advanced Research in Numerical Heat Transfer* 10, no. 1 (2022): 1-7.
- [35] Shit, G. C., M. Roy, and A. Sinha. "Mathematical modelling of blood flow through a tapered overlapping stenosed artery with variable viscosity." *Applied Bionics and Biomechanics* 11, no. 4 (2014): 185-195. <https://doi.org/10.1155/2014/698750>